HHS Public Access

Author manuscript

Colloids Surf A Physicochem Eng Asp. Author manuscript; available in PMC 2023 January 20.

Published in final edited form as:

Colloids Surf A Physicochem Eng Asp. 2022 September 05; 648: . doi:10.1016/j.colsurfa.2022.129147.

Modifying surface charge density of thermoplastic nanofluidic biosensors by multivalent cations within the slip plane of the electric double layer

Zheng Jia[a,d,1], **Junseo Choi**[a,d,1], **Sunggun Lee**[a,d,2], **Steven A. Soper**[b,c,d], **Sunggook Park**[a,d,*]

[a]Mechanical & Industrial Engineering Department, Louisiana State University, Baton Rouge, LA 70803, USA

[b]Department of Chemistry, University of Kansas, Lawrence, KS 66047, USA

[c]Department of Kansas Biology and KUCC, University of Kansas Medical Center, Kansas City, KS 66160, USA

[d]Center for Bio-Modular Multiscale Systems for Precision Medicine (CBM^2), USA

Abstract

Thermoplastic nanofluidic devices are promising platforms for sensing single biomolecules due to their mass fabrication capability. When the molecules are driven electrokinetically through nanofluidic networks, surface charges play a significant role in the molecular capture and transportation, especially when the thickness of the electrical double layer is close to the dimensions of the nanostructures in the device. Here, we used multivalent cations to alter the surface charge density of thermoplastic nanofluidic devices. The surface charge alteration was done by filling the device with a multivalent ionic solution, followed by withdrawal of the solution and replacing it with KCl for conductance measurement. A systematic study was performed using ionic solutions containing Mg^{2+} and Al^{3+} for nanochannels made of three polymers: poly(ethylene glycol) diacrylate (PEGDA), poly(methyl methacrylate) (PMMA) and cyclic olefin copolymer (COC). Overall, multivalent cations within the slip plane decreased the effective surface charge density of the device surface and the reduction rate increased with the cation valency, cation

*Correspondence to: Louisiana State University, Baton Rouge, LA 70803, USA. sunggook@lsu.edu (S. Park).

[1]Z.J and J.C contributed equally to this work

[2]SL worked as high school summer student intern from Baton Rouge Magnet High School. Current affiliation: College of Engineering, Duke University

CRediT authorship contribution statement

Zheng Jia: Investigation, Methodology, Writing – original draft preparation, **Junseo Choi**: Investigation, Methodology, Writing – orig- inal draft preparation, **Sunggun Lee**: Investigation, **Steven A. Soper**: Writing – reviewing and editing, **Sunggook Park**: Supervision, Conceptualization, Writing – reviewing and editing.

Supporting Information

Supporting information including thermoplastic nanofluidic devices fabrication steps, SEM images of nanochannels and in-plane nanopore, optical images of completely filled nanochannel device, nanochannel conductance as a function of withdraw-and-refill cycles during Al^{3+} modification and nanochannel conductance in two hours post modification is available in the online version of this article at http:

Declaration of Competing Interest

The authors declare that they have no known competing financial interests or personal relationships that could have appeared to influence the work reported in this paper.

Appendix A. Supporting information

Supplementary data associated with this article can be found in the online version at doi:10.1016/j.colsurfa.2022.129147.

concentration and the surface charge density of thermoplastic substrates. We demonstrated that a 10-nm diameter in-plane nanopore formed in COC allowed translocation of λ-DNA molecules after Al^{3+} modification, which is attributed to the deceased viscous drag force in the nanopore by the decreased surface charge density. This work provides a general method to manipulate surface charge density of nanofluidic devices for biomolecule resistive pulse sensing. Additionally, the experimental results support ion-ion correlations as the origin of charge inversion over specific chemical adsorption.

Graphical Abstract

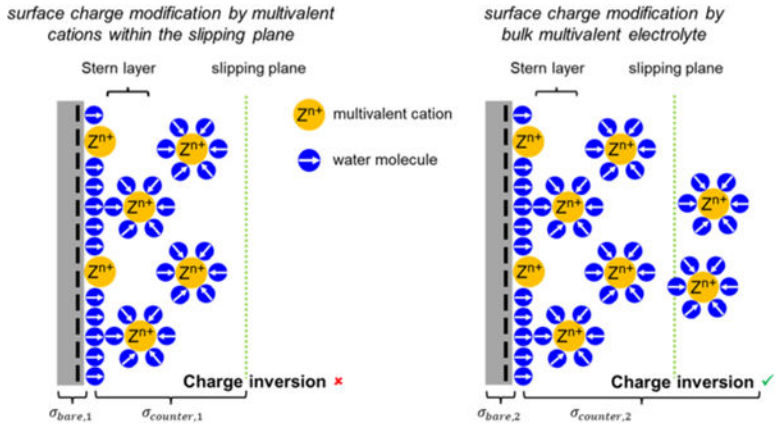

Keywords

Multivalent ions; Charge inversion; Thermoplastic nanofluidics; Nanopore; DNA translocation; Biomolecule sensing

1. Introduction

Unique transport phenomena and the capability of high sensitivity sensing in nanoscale confinement have made nanofluidic devices such as nanochannels [1, 2] and nanopores [3] ideal platforms for single-molecule analysis. In nanofluidic sensing applications, single molecules such as DNAs are introduced into the nanochannel or nanopore and their physiochemical properties are measured optically and electrically [4–7]. Thus, one of the most important prerequisites is to design the device structure and material that facilitate filling of fluid/reagents and driving of single molecules into the nanostructures. The rate of molecules driven into the nanostructures depends on the geometries, dimensions, and chemical properties of the nanostructures contained within the nanofluidic device as well as molecules to be transported through the device [8–10].

Recently, nanofluidic devices made of thermoplastics such as poly (methyl methacrylate) (PMMA) [11], cyclic olefin copolymer (COC) [12] and polycarbonate (PC) [13] have drawn tremendous attention as alternative candidates to replace silicon (Si)- and glass-based nanofluidic devices due to their low-cost and large-scale fabrication capability. However, the hydrophobic nature of most pristine thermoplastic substrates prevents easy filling of fluids and reagents into the nanostructures. To overcome this limitation, surface modification of

thermoplastic polymers via O_2 plasma or UV/O_3 treatment has routinely been performed [14–16], which improves the wetting of the substrate by increasing the surface energy. The modified hydrophilic surface also prevents biofouling by analytes such as DNAs, RNAs, proteins or cells during fluidic operation because of the low polymer-water interfacial energy [17]. Despite such advantages, O_2 plasma or UV/O_3 treatment also makes the device surfaces more negatively charged, which often plays a detrimental role affecting the rate of entry of single molecules into the nanostructures, especially when the physical size of the nanostructure is comparable to the electrical double layer thickness [8,18]. In such cases, the ability to modify the surface charge after the cover plate bonding of nanofluidic devices will enable easy entry of biomolecules into the nanostructures.

Surface charge density is a key material property of nanofluidic devices related to the ionic and molecular transport in the nanostructures [19–21] and thus the ability of controlling the surface charge density is critical to the design and fabrication of nanofluidic biosensors [8, 18, 22–24]. When a negatively charged (anionic) molecule is electrokinetically driven into a nanofluidic device with negative surface charges, the negative surface charges lead to a strong electroosmotic flow (EOF), which is opposite to the molecular motion by electrophoresis (EP). Therefore, the anionic molecule can be driven into the nanostructure electrophoretically only when the force by EP (F_{EP}) is larger than the viscous drag force by the EOF (F_{EOF}), and thus $F_{eff} = F_{EP} - F_{EOF} > 0$ [8, 9, 25, 26]. Here, F_{eff} is the effective driving force. Surface charge density of a device not only determines the direction and magnitude of EOF but also modifies the electric field strength in the nanostructures, affecting both F_{EOF} and F_{EP}, thus F_{eff} [8]. The more negative charges on the polymer substrate result in greater F_{EOF}, which may lead to an insufficient F_{eff} for molecules to overcome the entropy barrier [27–30] to the nanostructure. Our group experimentally demonstrated that double-stranded λ-DNA could only be translocated through in-plane nanopores when the device was made of polymers with low surface charge density, which also agreed well with the F_{eff} obtained by COMSOL simulation with the same device structure [8]. The results indicated that polymer nanofluidic devices with low surface charge density were desirable for single molecule analysis and that the ability to control the device surface charge density is critical to keep the rate of entry of single molecules into the nanofluidic sensors.

There are several ways to manipulate surface charge density of nanofluidic devices [31,32]. Inorganic and organic coatings via methods such as atomic layer deposition (ALD), layer-by-layer self-assembly and silanization could modify surface charge density and surface morphology of nanofluidic devices permanently [33]. Al_2O_3 [34] and HfO_2 [35] have been deposited on solid-state nanopores using ALD to fine-tune nanopore surface charge density, pore size and thus translocation performance. Various surface modification methods specifically for nanopore sensing applications can be found in an excellent recent review paper by Eggenberger et al. [33] Poly(ethylene glycol) (PEG) has been successfully grafted onto various substrates, such as Si_3N_4 [36], PMMA [14,37] and polydimethylsiloxane (PDMS) [38], to suppress EOF and biofouling. pH-tunable zwitterionic polymer brushes were grafted on polyimide (PI) conical nanopores to manipulate surface charges and thus current rectifications [39]. Compared to the above-mentioned techniques, dynamic coatings by surfactants or adding multivalent metal containing salt to the existing buffer is more

convenient, flexible, and cost-effective. Polyvinylpyrrolidone (PVP) has been used mostly for Si- or glass-based nanofluidic devices [40–42].

However, the existence of surfactant in the carrier buffer may affect the accuracy of biomolecule analysis based on resistive-pulse sensing (RPS) and mass spectrometry [14]. Another way to modify the substrate surface charge is by introducing multivalent metal salts directly into the carrier buffer[43,44]. Unlike commonly used monovalent electrolytes (such as KCl [45], NaCl [46] and LiCl [47]) for biomolecule RPS, both numerical and experimental studies demonstrated that multivalent cations can reduce or even invert the effective surface charge density of silica [48], glass [44] and polyimide [49] substrates and thus are good candidates for surface charge alteration of polymer nanofluidic devices. Multivalent ions play important roles in many cellular physiology and functions [50]. For example, Mg^{2+} stabilizes polyphosphate compounds in biological cells and acts as a cofactor of many enzyme reactions [51, 52]. Therefore, understanding of how the presence of multivalent ions affects the physiochemical properties of the device surface and the resultant rate of entry and transport of single molecules through nanostructures is critical toward the development of polymer nanofluidic biosensors.

In this study, we modified surface charge density of polymer nanofluidic devices to facilitate biomolecule translocation by using different multivalent cations: bivalent cation, Mg^{2+}, and trivalent cation, Al^{3+}. Unlike previous studies [44, 48, 49, 53, 54] where multivalent cations were used in carrier buffer directly, multivalent cations were used to pretreat the slip plane of the device surface and the mobile cations in the diffuse layer were replaced by the carrier buffer solution for either fluorescence observation (e.g., TE buffer) or ionic current measurement (e.g., 1 M KCl solution). The surface modification process used in this study is shown in Fig. 1a. Multivalent cation modifications were applied to nanochannels made of three polymer substrates via nanoimprint lithography: cyclic olefin copolymers (COC), poly(methyl methacrylate) (PMMA), and poly(ethylene glycol) diacrylate (PEGDA). The imprinted devices were then bonded to thin COC cover plates. It should be noted that prior to bonding the imprinted COC and PMMA substrates were treated with O_2 plasma while PEGDA substrates were bonded without O_2 plasma treatment. The bonded devices are denoted as COC-COC (substrate-cover plate), PMMA-COC and PEGDA-COC, respectively. In this way, fair comparison on the effect of surface charge alteration by multivalent cations could be made. Besides, the electrostatic properties of biomolecules remained unchanged when differently treated device surfaces were used. We also studied the effect of surface charge alteration by multivalent cations on adsorption and translocation of DNA molecules through thermoplastic in-plane nanopores.

2. Materials and methods

2.1. Fabrication of polymer nanochannels

Surface charge modification by Al^{3+} was conducted on nanofluidic devices made of three polymer substrates: cyclic olefin copolymers (COC), poly(methyl methacrylate) (PMMA), and poly(ethylene glycol) diacrylate (PEGDA). Their effective surface charge density was in a decreasing order of COC (more negative) > PMMA > PEGDA (less negative), as reported in our previous work [8]. Nanofluidic devices used for conductance measurements consisted

of five nanochannels with the width, height and length of 154 nm, 203 nm and 20 μm, respectively, and were fabricated on target substrates via thermal (COC and PMMA) and UV (PEGDA) nanoimprint lithography (NIL) at different imprinting conditions. The imprinted devices were then bonded to thin COC cover plates. Prior to bonding, the imprinted COC and PMMA substrates were treated with O_2 plasma for 30 s while no O_2 plasma treatment was performed for PEGDA substrates. The bonded devices are denoted as COC-COC (substrate-cover plate), PMMA-COC and PEGDA-COC, respectively. Details on the device fabrication can be found in our previous works [8, 55, 56]. Supporting information Fig. S1 describes fabrication steps for the polymer nanofluidic devices. SEM images of Si master mold and imprinted nanochannels on PEGDA, PMMA and COC are shown in Fig. 2a and Fig. S2a-d.

2.2. Surface charge modification by multivalent cations

For surface charge modification of polymer nanofluidic devices, $MgCl_2$ (Sigma-Aldrich) and $AlCl_3$ (Sigma-Aldrich) were used as model bivalent and trivalent salts, respectively. The step-by-step surface modification process is illustrated in Fig. 1. Nanofluidic devices were filled from one side of the microchannels via capillary force. After the microchannel was wet, the nanochannels were filled spontaneously by the capillary force. Before each conductance measurement, the device was inspected to make sure that all the nanochannels were wet and no air bubbles were trapped at nanochannel/funnel inlet interfaces, as presented in Fig. S3. We first measured the conductance of nanochannels filled with 10^{-6} M KCl (pH 7.0, Tris-HCl) as a baseline. For multivalent ion modification, the KCl solution in the nanochannel was withdrawn by a vacuum pump and the device was filled with a multivalent salt ($MgCl_2$ or $AlCl_3$) solution of a certain concentration (e.g. 10 mM, 100 mM, 500 mM and 1 M). After modification, the multivalent salt solution was withdrawn by a vacuum pump and the mobile multivalent cations outside the slip plane were replaced by K^+ through withdraw-and-refill cycles with 10^{-6} M KCl solution.

Nanochannel conductance was measured every four withdraw-and-refill cycles. The conductance decreased as the multivalent salt solution in the nanochannel was replaced by KCl solution. We stopped the withdraw-and-refill process when the measured conductance value became stable. Then we proceeded to the next multivalent ion concentration. For each type of multivalent salt solution, conductance measurements were performed on eight nanofluidic devices. Axopatch 200B (Molecular Devices) was used for conductance measurements. As documented in Fig. S4, when modified by Al^{3+}, the nanochannel conductance tended to saturate from the fourth withdraw-and-refill cycle. The modification was stable while a continuous conductance measurement under 1 V bias for two hours was performed, as recorded in Table S1.

2.3. Translocation of λ-DNA through Al^{3+} modified COC in-plane nanopore

Prior to DNA translocation experiment, the binding behavior of negatively charged DNA to Al^{3+} modified COC-COC devices was studied for devices modified with different concentrations of $AlCl_3$ solutions (0 M, 10 mM, 100 mM, 500 mM and 1 M). 5 ng/μL λ-DNA (New England BioLabs) stained with YOYO-1 (ThermoFisher Scientific) was introduced into COC microchannels. DNA solution was withdrawn after 2 min and the

microchannel was rinsed with 1× TE buffer (Sigma-Aldrich, containing 10 mM Tris-HCl, 1 mM EDTA, pH 8.0). DNA molecules binding to microchannel walls was observed by a fluorescence microscope (Olympus IX70) with a 100× oil immersion objective (Olympus). Fluorescence images were captured by a CCD camera (Photon Max, Princeton Instruments) and the number of binding molecules on the microchannel surface was counted using the ImageJ software (National Institutes of Health).

DNA translocation experiments were conducted in a COC nanofluidic device containing an in-plane nanopore with 10-nm diameter (equivalent diameter after thermal fusion bonding) before and after 100 mM $AlCl_3$ modification. SEM images of the in-plane nanopore device are shown in Fig. 2b, Fig. S5 and our previous work [8,57]. 1× TE was filled into the nanopore device as buffer and then a solution of 5 ng/μL double-strand λ-DNA stained with YOYO-1 dye was added to the cis side of the microchannel. Pt electrodes were used to drive DNA molecules with a commercial power supply (BK Precision DC power supply 1735).

3. Results and discussion

3.1. COC surface charge modification by $MgCl_2$ and $AlCl_3$

To quantify the variation of surface charge density of the polymer nanochannel walls upon multivalent ion modification, we measured the nanochannel conductance in the presence of 10^{-6} M KCl before and after the modification. With 10^{-6} M KCl, the corresponding Debye length is ~ 300 nm, significantly larger than the width and depth of the nanochannels. At such low salt concentration, the nanochannel conductance, G_s, is governed by the number of mobile charge carriers inside the nanochannel, which is proportional to the substrate effective surface charge density [58], σ_{eff}, as given by,

$$G_s = 2\mu_{opp} \times \sigma_{eff} \times n \times (w + h)/L \quad (1)$$

where n is the number of nanochannels in the device. w, L and h are the nanochannel width, length and height, respectively. μ_{opp} is the mobility of the counterion and σ_{eff} is the effective surface charge density.

σ_{eff} of a nanochannel wall is defined as the charge density exerted at the slip plane in the electrical double layer and thus includes the effects of the surface charge density from the bare polymer surface, $-\sigma_{\text{bare}}$, and immobilized counterions within the slip plane, σ_{counter}, as given by

$$\sigma_{eff} = -\sigma_{bara} + \sigma_{counter} \quad (2)$$

Based on strongly correlated liquid (SLC) theory, as bulk multivalent electrolyte concentration increases, the absolute value of σ_{eff} will decrease and then increase again after charge inversion [48,59]. Accordingly, the measured nanochannel conductance at low KCl concentration is expected to decrease as multivalent cations start to bind to the surface and then increase again upon further binding after surface charge inversion.

Fig. 3a and b show nanochannel conductance with 10^{-6} M KCl solution after the nanochannel surface was modified by different concentrations of $MgCl_2$ and $AlCl_3$ solutions, respectively. For each measured conductance, the surface charge density was estimated simply using Eq. (1) with the following experimental parameters: w = 154 nm, h = 203 nm, L = 20 μm, n = 5 and μ_{opp} = 7.619 10^{-8} $m^2V^{-1}s^{-1}$ (K^+ as counter ions). The use of this equation in the estimation of surface charge density can be justified because a sufficiently low KCl concentration (10^{-6} M) was used to measure the conductance.

Overall, the measured conductance decreased dramatically as the multivalent ion concentration increased to 100 mM, which is followed by a slight decrease as the ion concentration further increased. The decrease in conductance indicates binding of multivalent ions to the negatively charged COC surface, leading to a decrease in σ_{eff}. It should be noted that charge inversion did not occur. The surface modification by Al^{3+} ions resulted in more dramatic decreases in conductance due to a stronger electrostatic interaction with the negatively charged COC surface as shown in the insets of Fig. 3. The results agree with previous studies, where bivalent cations are less effective to screen [48] or invert [49] the surface charge because of their lower Gibbs free energy of ion hydration [44,60] or weaker binding energy [61].

Charge inversion or overcharging occurs on surfaces with high surface charge density in the presence of multivalent ions [62] and was experimentally observed on silica [48], glass [44] and polyimide [49] substrates. For glass substrates, the charge inversion concentration, c_{inv}, was as low as 0.5 mM when $AlCl_3$ was used as the electrolyte[44]. The σ_{eff} of flat glass and silica plates with monovalent electrolytes ranged from − 0.2 to − 40 mC/m^2 at pH 7 [63,64]. The σ_{eff} of the COC-COC nanochannel in KCl ($\sigma_{eff,KCl}$ as indicated in Fig. 1a) was measured to be − 73.8 mC/m^2 [8], higher (more negative) than that for glass and silica. However, in our experiment, we did not observe charge inversion even at an $AlCl_3$ concentration of 1 M. The main difference from previous studies is that, in our work, after the device surface was modified with multivalent cations the mobile cations in the diffuse layer were replaced by K^+ ions, so that the multivalent cations were only confined within the slip plane. In previous studies where charge inversion was observed, the multivalent cations are present beyond the slip plane, which may impact the effective surface charges [62]. According to Lyklem [62,65], it is still an open question if overcharging (charge inversion) of a surface in multivalent electrolytes would take place beyond the slip plane. If the binding of Al^{3+} to the negatively charged COC surface is much stronger than the binding of K^+ to the same surface and thus that the counterions distribution within the slip plane (which forms a sharp boarder separating the mobile from immobile counterions) remains unchanged upon replacing the residual Al^{3+} ions by K^+ ions, our results support the hypothesis that overcharging takes place beyond the slip plane. This also indicates that ion-ion correlations would be the dominant contributor for overcharging compared to specific chemical adsorption [62, 65, 66].

Comparing Fig. 3a and b, Al^{3+} reduced the COC surface charge density more efficiently than Mg^{2+}, which can be attributed to its stronger binding energy to the negatively charged polymer surface [61], and it is in good agreement with previous numerical [59,61] and experimental [43, 44, 67, 68] studies. In a similar manner, polymer substrates with higher

(more negative) surface charge density can be screened more effectively by the same multivalent ions, leading to greater surface charge reduction rates [68]. Our previous work showed that before multivalent cation modification, the magnitude of $\sigma_{\text{eff, KCl}}$ increased in the order PEGDA-COC < PMMA-COC < COC-COC devices, with $\sigma_{\text{eff, KCl}}$ being − 24.1, − 51.7, and − 73.8 mC/m^2, respectively [8]. For those polymer devices, we evaluated the effect of the substrate surface charge density on the magnitude of the surface charge modification by Al^{3+} ions, which is shown in Fig. 4a and b. For all the polymer nanochannels, the conductance rapidly decreased at lower $AlCl_3$ concentration, which then showed an attenuated decreasing rate as the $AlCl_3$ concentration increased. Fig. 4b shows the surface charge reduction rate upon $AlCl_3$ modification versus the effective surface charge density, $\sigma_{\text{eff,KCl}}$, of different polymers prior to the modification; the Al^{3+} modified COC-COC and PEGDA-COC devices showed the largest and smallest reductions, respectively. In general, nanochannels with more negative surface charge prior to multivalent cation modification resulted in more surface charge reduction, which is attributed to the stronger electrostatic attraction to the counterions.

While our analysis considered the electrostatics aspect only with the assumption that binding of multivalent ions to the surface is much stronger than the binding of monovalent K^+ ions, adsorption of ions on a surface is not an irreversible process and depends not only on the valence but also other factors such as ion radius and surface charge [69]. In general, the smaller cation or the multivalent cation is preferentially adsorbed at the negatively charged surface [69]. The ionic radii of K^+, Mg^{2+}, and Al^{3+} in water are 1.33, 0.65, and 0.50 Å, respectively, and their hydration radii are 3.3, 4.3, and 4.8 Å, respectively [69,70]. The multivalent ions used in this study are slightly larger in hydration radius than K^+. The Monte Carlo simulation and density functional theory results by Valisko et al. shows that when the ionic diameter and valence competes in ionic adsorption, the electrostatic advantage of the multivalent ions dominates at lower surface charges, whereas at higher surface charges the entropic advantage of the small ions dominates [69]. In their study, when monovalent ions with a diameter of 2 Å and divalent ions with a diameter of 4.24 Å are competing in adsorption at a negatively charged surface, adsorption of the small monovalent ions dominated at the surface charges larger than − 900 mC/m^2. When divalent cations are smaller than monovalent cations, adsorption of small divalent cations dominated irrespectively of the surface charge. Because the surface charges of polymer substrates used in this study are relatively small, our assumption of the preferential adsorption of Mg^{2+} and Al^{3+} over K^+ and the analysis based on the electrostatics aspect can be justified.

3.2. Adsorption and translocation of λ-DNA through Al^{3+} modified COC in-plane nanopore

Strongly charged polyelectrolyte, for example dsDNA, binding to substrate surface with opposite charges has been studied extensively[61, 71]. We studied the effect of Al^{3+} modification on the adsorption and translocation of ds-λ-DNA using an in-plane nanopore device made of COC. Fig. 5a-e shows fluorescence images after 5 ng/μL λ-DNA stained with YOYO-1 was introduced into and withdrawn from COC-COC microchannels. Even though the results from the conductance measurements showed that the COC substrate after Al^{3+} modification (up to 1 M) still held a negative $\sigma_{\text{eff, AlCl3}}$, the number of DNA molecules

bound to the surface increased as the concentration of the $AlCl_3$ solution used for the surface charge modification increased. Interestingly, the plateau located close to the $AlCl_3$ concentration of 100 mM, which is consistent with the conductance measurement result in Fig. 3b. Besides, the results indicated that binding of Al^{3+} and the negatively charged bare COC substrate with O_2 plasma treatment is strong and that local overcharging [54] might cause the electrostatic binding of DNA.

We also tested how multivalent cation modification of the COC-COC device affected the translocation of λ-DNA molecules through an in-plane nanopore when the molecules were driven electrokinetically. In our previous study we could not observe any translocation of λ-DNA molecules through the COC-COC in-plane nanopore, which was attributed to the increased magnitude of F_{EOF} due to the high surface charge density leading to $F_{eff} < 0$[8]. Fig. 6 shows an optical micrograph of the COC-COC device with an in-plane nanopore and the fluorescence images of λ-DNA translocation through the device with and without the Al^{3+} modification taken with a 100× oil immersion lens. Note that the scale bar in the figure corresponds to 5 μm. Even though the image was not as sharp, the translocation, piling up, and stretching of DNA were identifiable. Prior to $AlCl_3$ modification, all incoming DNA molecules electrophoretically driven at a driving voltage of 800 mV piled up in front of the nanopore without any translocation. After the modification with 100 mM $AlCl_3$, the DNA molecules were driven toward the nanopore and passed through the nanopore under the same voltage bias. That can be explained by the reduced magnitude of F_{EOF} due to the lowering of σ_{eff} on the nanopore wall.

Even though COC-COC devices were modified by $AlCl_3$ solution with a moderate concentration, some binding of DNA molecules was observed especially on the pillar structures designed for DNA pre-stretching prior to the nanopore. Compared to the DNA binding study conducted in the microchannel (Fig. 5), the more confined geometry in the nanopillar region, thus higher surface-to-volume ratio, seemed to increase the DNA binding. This DNA binding may be associated with the enhanced attraction of DNA molecules mediated by multivalent ions existing within the slip plane [72]. Thus, the use of multivalent cations to enhance translocation in nanofluidics may require selection of cations with appropriate valence and ionic strength, careful design of micro/nanostructures in the device, and determination of optimal electrokinetic conditions for the translocation.

The presence of multivalent ions in the nanopore or nanochannel devices is known to affect the translocation behavior of biomolecules. When multivalent ions, for example Mg^{2+}, were added to buffer solution directly, the translocation velocity of DNA through nanopores was reduced due to stronger screening of counterions at both the nanopore surface and the chain of the DNA molecules [46,53]. The decreased effective surface charge density on the negative DNA strand leads to a decrease in the DNA electrophoretic velocity. Introducing multivalent cations within the slip plane only, as demonstrated in this work, would increase the counterion screening at the nanopore surface, but the counterion screening on the DNA molecules remains unchanged. Therefore, while F_{EP} on the DNA molecule remains similar, the decreased effective surface charge density at the nanopore wall reduces F_{EOF}, which would lead to a higher DNA translocation velocity compared to the use of KCl buffer or adding multivalent salt to the buffer directly. The optimal electrokinetic conditions for

biomolecule translocation will be determined depending on the target application, and the multivalent ion modification that is presented in this work may be useful for applications where an increased translocation velocity is desired. One example of such applications includes exonuclease sequencing where an increased velocity of mononucleotides clipped from DNA/RNA via enzymatic reaction would reduce diffusional misordering of chipped mononucleotides before entering into the nanopore sensor [73]. Binding of DNA molecules at the wall of nanopore may also affect the translocation velocity. In our work, however, DNA binding was mostly observed at the pillar array region prior to the in-plane nanopore. It would be an interesting research topic to study the effect of DNA binding to the nanopore surface on the translocation velocity of subsequent DNAs.

It should be noted that the stability of the modified surface is critical to use this surface modification method for various applications. Table S1 of the Supplementary information shows the time-dependent conductance of 10^{-6} M KCl up to 2 h after modifying the COC nanochannels by 500 mM $AlCl_3$ solution. After 2 h, only 3% of conductance variation was observed, indicating a stability of the multivalent ion modification during this period. While such stability can be attributed to a strong short-range electrostatic force between the multivalent ions and the surface charges, the long-term stability needs to be further investigated in the future.

4. Conclusions

In this work, we present a general method to modify the surface charge density in polymer nanofluidic devices by using multivalent cations. After filling the nanochannels with a multivalent electrolyte, the electrolyte was withdrawn and replaced with KCl, so that the bare surface charges on the polymer substrate were screened only by the stagnant multivalent cations within the slip plane. We found that the extent of the surface charge modification is dependent on the valency of cations and the charge density of the polymer substrates. Compared with Mg^{2+}, Al^{3+} reduced the surface charge of polymer nanochannels more efficiently. Despite the reduction, no charge inversion was observed for Al^{3+} modified COC. Overcharging in electrical double layers have been observed when multivalent ions are present in both the stagnant and diffuse layer. Our results associated with the absence of detectable overcharging in highly negatively charged polymer substrates may indicate that overcharging in the electrical double layer takes place beyond the slip plane and that ion-ion correlations would be the dominant contributor for overcharging over specific chemical adsorption. Surface charge reduction by Al^{3+} was more effective for polymer substrate possessing more negatively charged surface. After Al^{3+} modification, we could translocate λ-DNA molecules through a COC-COC nanofluidic device equipped with an in-plane nanopore. However, electrostatic adsorption of λ-DNA molecules observed in the multivalent cation modified polymer substrate is an issue to be considered before implementing this technique for enhancing translocation of biomolecules in polymer nanofluidic devices.

Supplementary Material

Refer to Web version on PubMed Central for supplementary material.

Acknowledgments

The authors would like to thank the National Institutes of Health for funding of this work (NIBIB:P41 EB020594). The authors also thank the LSU Shared Instrumentation Facilities (SIF) and Center for Advanced Materials and Devices (CAMD) for assistance in performing focused ion beam milling and lithography, respectively, used in this work.

References

[1]. Foquet M, Korlach J, Zipfel W, Webb WW, Craighead HG, DNA fragment sizing by single molecule detection in submicrometer-sized closed fluidic channels, Anal. Chem 74 (2002) 1415–1422. [PubMed: 11922312]

[2]. Menard LD, Mair CE, Woodson ME, Alarie JP, Ramsey JM, A device for performing lateral conductance measurements on individual double-stranded DNA molecules, ACS Nano 6 (2012) 9087–9094. [PubMed: 22950784]

[3]. Harms ZD, Mogensen KB, Nunes PS, Zhou K, Hildenbrand BW, Mitra I, Tan Z, Zlotnick A, Kutter JP, Jacobson SC, Nanofluidic devices with two pores in series for resistive-pulse sensing of single virus capsids, Anal. Chem 83 (2011) 9573–9578. [PubMed: 22029283]

[4]. Howorka S, Siwy Z, Nanopores and nanochannels: from gene sequencing to genome mapping, ACS Nano 10 (2016) 9768–9771. [PubMed: 27934066]

[5]. Xiao K, Wen L, Jiang L, Biomimetic solid-state nanochannels: from fundamental research to practical applications, Small 12 (2016) 2810–2831. [PubMed: 27040151]

[6]. Laucirica G, Terrones YT, Cayón V, Cortez ML, Toimil-Molares ME, Trautmann C, Marmisollé W, Azzaroni O, Biomimetic solid-state nanochannels for chemical and biological sensing applications, Trends Anal. Chem 144 (2021), 116425.

[7]. Pérez-Mitta G, Toimil-Molares ME, Trautmann C, Marmisollé WA, Azzaroni O, Molecular design of solid-state nanopores: fundamental concepts and applications, Adv. Mater 31 (2019), 1901483.

[8]. Jia Z, Choi J, Park S, Surface charge density-dependent DNA capture through polymer planar nanopores, ACS Appl. Mater. Interfaces 10 (2018) 40927–40937. [PubMed: 30371050]

[9]. He Y, Tsutsui M, Taniguchi M, Kawai T, DNA capture in nanopores for genome sequencing: challenges and opportunities, J. Mater. Chem 22 (2012) 13423–13427.

[10]. Wu J, Wang H, Kim J, Murphy F, Soper SA, Park S, Influence of nanochannel inlet structure upon DNA capture ratio. Proceedings of the ASME 2011 International Mechanical Engineering Congress and Exposition, American Society of Mechanical Engineers, 2011, pp. 643–645.

[11]. Uba FI, Pullagurla SR, Sirasunthorn N, Wu J, Park S, Chantiwas R, Cho YK, Shin H, Soper SA, Surface charge, electroosmotic flow and DNA extension in chemically modified thermoplastic nanoslits and nanochannels, Analyst 140 (2015) 113–126. [PubMed: 25369728]

[12]. Uba FI, Hu B, Weerakoon-Ratnayake K, Oliver-Calixte N, Soper SA, High process yield rates of thermoplastic nanofluidic devices using a hybrid thermal assembly technique, Lab Chip 15 (2015) 1038–1049. [PubMed: 25511610]

[13]. Kawano R, Osaki T, Sasaki H, Takeuchi S, A polymer-based nanopore-integrated microfluidic device for generating stable bilayer lipid membranes, Small 6 (2010) 2100–2104. [PubMed: 20839243]

[14]. Liu J, Pan T, Woolley AT, Lee ML, Surface-modified poly (methyl methacrylate) capillary electrophoresis microchips for protein and peptide analysis, Anal. Chem 76 (2004) 6948–6955. [PubMed: 15571346]

[15]. Wei S, Vaidya B, Patel AB, Soper SA, McCarley RL, Photochemically patterned poly (methyl methacrylate) surfaces used in the fabrication of microanalytical devices, J. Phys. Chem. B 109 (2005) 16988–16996. [PubMed: 16853163]

[16]. Chai J, Lu F, Li B, Kwok DY, Wettability interpretation of oxygen plasma modified poly (methyl methacrylate), Langmuir 20 (2004) 10919–10927. [PubMed: 15568841]

[17]. Krishnan S, Weinman CJ, Ober CK, Advances in polymers for anti-biofouling surfaces, J. Mater. Chem 18 (2008) 3405–3413.

[18]. He Y, Tsutsui M, Fan C, Taniguchi M, Kawai T, Gate manipulation of DNA capture into nanopores, ACS Nano 5 (2011) 8391–8397. [PubMed: 21928773]

[19]. Qiu Y, Lin C-Y, Hinkle P, Plett TS, Yang C, Chacko JV, Digman MA, Yeh L-H, Hsu J-P, Siwy ZS, Highly charged particles cause a larger current blockage in micropores compared to neutral particles, ACS Nano 10 (2016) 8413–8422. [PubMed: 27532683]

[20]. Wu Y, Qian Y, Niu B, Chen J, He X, Yang L, Kong XY, Zhao Y, Lin X, Zhou T, Surface charge regulated asymmetric ion transport in nanoconfined space, Small 17 (2021), 2101099.

[21]. Tian Y, Wen L, Hou X, Hou G, Jiang L, Bioinspired ion-transport properties of solid-state single nanochannels and their applications in sensing, ChemPhysChem 13 (2012) 2455–2470. [PubMed: 22715160]

[22]. Paik K-H, Liu Y, Tabard-Cossa V, Waugh MJ, Huber DE, Provine J, Howe RT, Dutton RW, Davis RW, Control of DNA capture by nanofluidic transistors, ACS Nano 6 (2012) 6767–6775. [PubMed: 22762282]

[23]. Venkatesan BM, Shah AB, Zuo JM, Bashir R, DNA sensing using nanocrystalline surface-enhanced Al2O3 nanopore sensors, Adv. Funct. Mater 20 (2010) 1266–1275. [PubMed: 23335871]

[24]. Siwy Z, Heins E, Harrell CC, Kohli P, Martin CR, Conical-nanotube ion-current rectifiers: the role of surface charge, J. Am. Chem. Soc 126 (2004) 10850–10851. [PubMed: 15339163]

[25]. Wong CT, Muthukumar M, Polymer capture by electro-osmotic flow of oppositely charged nanopores, J. Chem. Phys 126 (2007), 164903. [PubMed: 17477630]

[26]. Muthukumar M, Theory of capture rate in polymer translocation, J. Chem. Phys 132 (2010), 05B605.

[27]. Zhou J, Wang Y, Menard LD, Panyukov S, Rubinstein M, Ramsey JM, Enhanced nanochannel translocation and localization of genomic DNA molecules using three-dimensional nanofunnels, Nat. Commun 8 (2017) 807. [PubMed: 28993619]

[28]. Kumar R, Muthukumar M, Origin of translocation barriers for polyelectrolyte chains, J. Chem. Phys 131 (2009), 11B610.

[29]. Chen L, Conlisk A, Modeling of DNA translocation in nanopores In: Proceedings of the 47th AIAA Aerospace Sciences Meeting including The New Horizons Forum and Aerospace Exposition, 2009, pp. 1121.

[30]. van Dorp S, Keyser UF, Dekker NH, Dekker C, Lemay SG, Origin of the electrophoretic force on DNA in solid-state nanopores, Nat. Phys 5 (2009) 347–351.

[31]. Lin C-Y, Turker Acar E, Polster JW, Lin K, Hsu J-P, Siwy ZS, Modulation of charge density and charge polarity of nanopore wall by salt gradient and voltage, ACS Nano 13 (2019) 9868–9879. [PubMed: 31348640]

[32]. Pérez-Mitta G, Albesa AG, Trautmann C, Toimil-Molares ME, Azzaroni O, Bioinspired integrated nanosystems based on solid-state nanopores:“iontronic” transduction of biological, chemical and physical stimuli, Chem. Sci 8 (2017) 890–913. [PubMed: 28572900]

[33]. Eggenberger OM, Ying C, Mayer M, Surface coatings for solid-state nanopores, Nanoscale 11 (2019) 19636–19657. [PubMed: 31603455]

[34]. Chen P, Mitsui T, Farmer DB, Golovchenko J, Gordon RG, Branton D, Atomic layer deposition to fine-tune the surface properties and diameters of fabricated nanopores, Nano Lett 4 (2004) 1333–1337. [PubMed: 24991194]

[35]. Yamazaki H, Hu R, Zhao Q, Wanunu M, Photothermally assisted thinning of silicon nitride membranes for ultrathin asymmetric nanopores, ACS Nano 12 (2018) 12472–12481. [PubMed: 30457833]

[36]. Tang Z, Lu B, Zhao Q, Wang J, Luo K, Yu D, Surface modification of solid-state nanopores for sticky-free translocation of single-stranded DNA, Small 10 (2014) 4332–4339. [PubMed: 25044955]

[37]. Bi H, Meng S, Li Y, Guo K, Chen Y, Kong J, Yang P, Zhong W, Liu B, Deposition of PEG onto PMMA microchannel surface to minimize nonspecific adsorption, Lab Chip 6 (2006) 769–775. [PubMed: 16738729]

[38]. Kovach KM, Capadona JR, Gupta AS, Potkay JA, The effects of PEG-based surface modification of PDMS microchannels on long-term hemocompatibility, J. Biomed. Mater. Res. Part A 102 (2014) 4195–4205.

[39]. Yameen B, Ali M, Neumann R, Ensinger W, Knoll W, Azzaroni O, Single conical nanopores displaying pH-tunable rectifying characteristics. Manipulating ionic transport with zwitterionic polymer brushes, J. Am. Chem. Soc 131 (2009) 2070–2071. [PubMed: 19159287]

[40]. Kaneta T, Ueda T, Hata K, Imasaka T, Suppression of electroosmotic flow and its application to determination of electrophoretic mobilities in a poly (vinylpyrrolidone)-coated capillary, J. Chromatogr. A 1106 (2006) 52–55. [PubMed: 16443452]

[41]. Milanova D, Chambers RD, Bahga SS, Santiago JG, Effect of PVP on the electroosmotic mobility of wet-etched glass microchannels, Electrophoresis 33 (2012) 3259–3262. [PubMed: 23065690]

[42]. Menard LD, Ramsey JM, Electrokinetically-driven transport of DNA through focused ion beam milled nanofluidic channels, Anal. Chem 85 (2012) 1146–1153. [PubMed: 23234458]

[43]. Chou K-H, McCallum C, Gillespie D, Pennathur S, An experimental approach to systematically probe charge inversion in nanofluidic channels, Nano Lett 18 (2018) 1191–1195. [PubMed: 29266955]

[44]. Brechtel R, Hohmann W, Rüdiger H, H. Wätzig, Control of the electroosmotic flow by metal-salt-containing buffers, J. Chromatogr. A 716 (1995) 97–105.

[45]. Storm AJ, Storm C, Chen J, Zandbergen H, Joanny J-F, Dekker C, Fast DNA translocation through a solid-state nanopore, Nano Lett 5 (2005) 1193–1197. [PubMed: 16178209]

[46]. Uplinger J, Thomas B, Rollings R, Fologea D, McNabb D, Li J, K+ , N a+, and M g2+ on DNA translocation in silicon nitride nanopores, Electrophoresis 33 (2012) 3448–3457. [PubMed: 23147752]

[47]. Kowalczyk SW, Wells DB, Aksimentiev A, Dekker C, Slowing down DNA translocation through a nanopore in lithium chloride, Nano Lett 12 (2012) 1038–1044. [PubMed: 22229707]

[48]. Van der Heyden FH, Stein D, Besteman K, Lemay SG, Dekker C, Charge inversion at high ionic strength studied by streaming currents, Phys. Rev. Lett 96 (2006), 224502. [PubMed: 16803311]

[49]. Ramirez P, Manzanares JA, Cervera J, Gomez V, Ali M, Pause I, Ensinger W, Mafe S, Nanopore charge inversion and current-voltage curves in mixtures of asymmetric electrolytes, J. Membr. Sci 563 (2018) 633–642.

[50]. Liu Q, Wen L, Xiao K, Lu H, Zhang Z, Xie G, Kong XY, Bo Z, Jiang L, Biomimetic A, Voltage-gated chloride nanochannel, Adv. Mater 28 (2016) 3181–3186. [PubMed: 26917448]

[51]. Oliver-Calixte NJ, Uba FI, Battle KN, Weerakoon-Ratnayake KM, Soper SA, Immobilization of Lambda exonuclease onto polymer micropillar arrays for the solid-phase digestion of dsDNAs, Anal. Chem 86 (2014) 4447–4454. [PubMed: 24628008]

[52]. Pilchova I, Klacanova K, Tatarkova Z, Kaplan P, Racay P, The involvement of Mg2+ in regulation of cellular and mitochondrial functions, Oxid. Med. Cell. Longevity 2017 (2017), 6797460.

[53]. Zhang Y, Liu L, Sha J, Ni Z, Yi H, Chen Y, Nanopore detection of DNA molecules in magnesium chloride solutions, Nanoscale Res. Lett 8 (2013) 245. [PubMed: 23688283]

[54]. Lin K, Lin C-Y, Polster JW, Chen Y, Siwy ZS, Charge inversion and calcium gating in mixtures of ions in nanopores, J. Am. Chem. Soc 142 (2020) 2925–2934. [PubMed: 31964139]

[55]. Jia Z, Choi J, Park S, Selection of UV resins for nanostructured molds for thermal- NIL, Nanotechnology 29 (2018), 365302. [PubMed: 29911991]

[56]. Choi J, Jia Z, Park S, Fabrication of polymeric dual-scale nanoimprint molds using a polymer stencil membrane, Microelectr. Eng 199 (2018) 101–105.

[57]. Choi J, Jia Z, Riahipour R, McKinney CJ, Amarasekara CA, Weerakoon- Ratnayake KM, Soper SA, Park S, Label-free identification of single mononucleotides by nanoscale electrophoresis, Small 17 (2021), 2102567.

[58]. Schoch RB, Renaud P, Ion transport through nanoslits dominated by the effective surface charge, Appl. Phys. Lett 86 (2005), 253111.

[59]. Shklovskii BI, Screening of a macroion by multivalent ions: correlation-induced inversion of charge, Phys. Rev. E 60 (1999) 5802.

[60]. Zimmermann R, Freudenberg U, Schweiß R, Küttner D, Werner C, Hydroxide and hydronium ion adsorption – a survey, Curr. Opin. Colloid Interface Sci 15 (2010) 196–202.

[61]. Quesada-Pérez M, González-Tovar E, Martín-Molina A, Lozada-Cassou M, Hidalgo-Álvarez R, Overcharging in colloids: beyond the Poisson–Boltzmann approach, ChemPhysChem 4 (2003) 234–248. [PubMed: 12674596]

[62]. Lyklema J, Quest for ion–ion correlations in electric double layers and overcharging phenomena, Adv. Colloid Interface Sci 147 (2009) 205–213. [PubMed: 19162256]

[63]. Behrens SH, Grier DG, The charge of glass and silica surfaces, J. Chem. Phys 115 (2001) 6716–6721.

[64]. Barisik M, Atalay S, Beskok A, Qian S, Size dependent surface charge properties of silica nanoparticles, J. Phys. Chem. C 118 (2014) 1836–1842.

[65]. Lyklema J, Overcharging, charge reversal: chemistry or physics? Colloids Surf. A: Physicochem. Eng. Asp 291 (2006) 3–12.

[66]. de Vos WM, Lindhoud S, Overcharging and charge inversion: finding the correct explanation (s), Adv. Colloid Interface Sci 274 (2019), 102040. [PubMed: 31698305]

[67]. Besteman K, Van Eijk K, Lemay S, Charge inversion accompanies DNA condensation by multivalent ions, Nature Physics 3 (2007) 641.

[68]. Besteman K, Zevenbergen MA, Heering HA, Lemay SG, Direct observation of charge inversion by multivalent ions as a universal electrostatic phenomenon, Phys. Rev. Lett 93 (2004), 170802. [PubMed: 15525062]

[69]. Valiskó M, Boda D, Gillespie D, Selective adsorption of ions with different diameter and valence at highly charged interfaces, J. Phys. Chem. C 111 (2007) 15575–15585.

[70]. Doi A, Khosravi M, Ejtemaei M, Nguyen TAH, Nguyen AV, Specificity and affinity of multivalent ions adsorption to kaolinite surface, Appl. Clay Sci 190 (2020), 105557.

[71]. Grosberg AY, Nguyen T, Shklovskii B, Colloquium: the physics of charge inversion in chemical and biological systems, Rev. Mod. Phys 74 (2002) 329.

[72]. Allahyarov E, Gompper G, Lowen H, Attraction between DNA molecules mediated by multivalent ions, Phys. Rev. E 69 (2003), 041904.

[73]. Reiner JE, Balijepalli A, Robertson JWF, Drown BS, Burden DL, Kasianowicz JJ, The effects of diffusion on an exonuclease/nanopore-based DNA sequencing engine, J. Chem. Phys 137 (2012), 214903. [PubMed: 23231259]

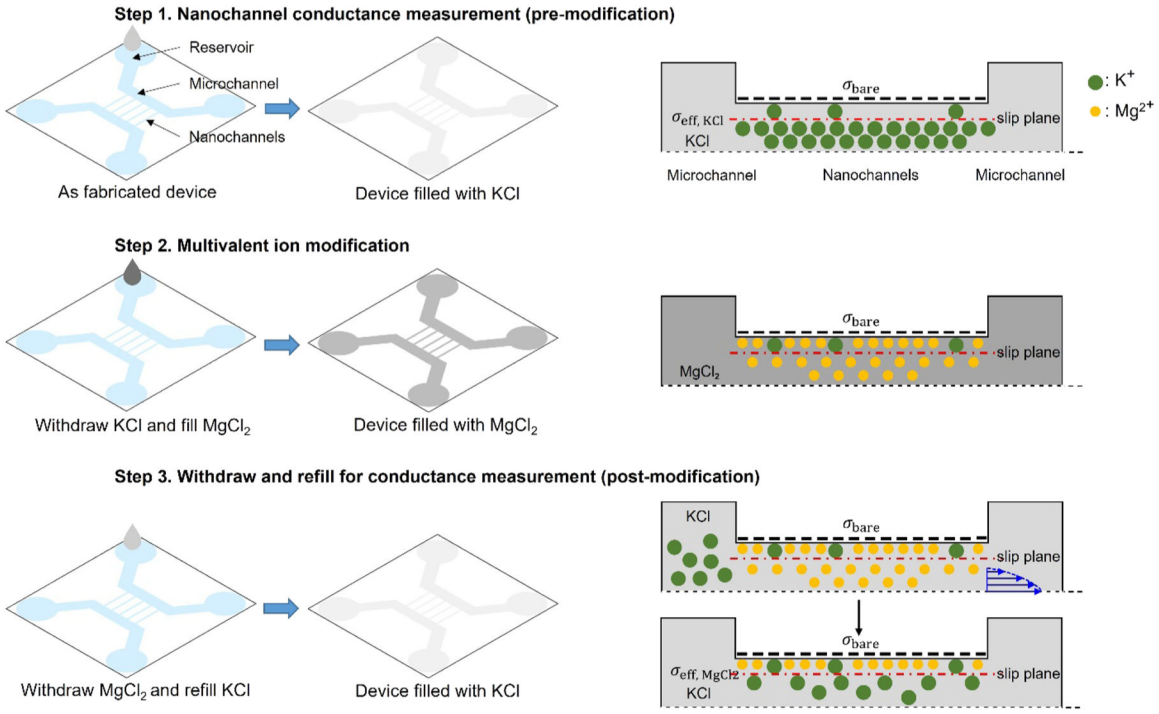

Fig. 1.

Surface modification process. The left panel describes how the electrolyte solution was introduced into the nanofluidic devices and the right panel presents schematics showing the changes of ion distribution inside the nanochannel (cross-section view along the channel). Step 1: Nanochannel conductance measurement before multivalent ion modification. A nanofluidic device was filled from one side of the microchannels with 10^{-6} M KCl. Once the microchannel was wet, the nanochannels were filled spontaneously by capillary force. From the measured conductance, $\sigma_{\text{eff, KCl}}$ was calculated as a baseline. Step 2: Surface modification by multivalent ions. The KCl solution in the nanofluidic device was withdrawn by a vacuum pump and the device was filled with multivalent electrolyte ($MgCl_2$ is shown as an example) having different concentrations. Step 3: Conductance measurement after modification. The mobile multivalent cations outside the slip plane were replaced with 10^{-6} M KCl by repeating withdrawal and refilling process multiple times. This step was monitored by measuring the nanochannel conductance every four withdraw-and-refill cycles. If the measured conductance was not saturated to a stable value (lower than the baseline), this step was repeated. $\sigma_{\text{eff, MgCl2}}$ was calculated from the saturated nanochannel conductance value after the modification.

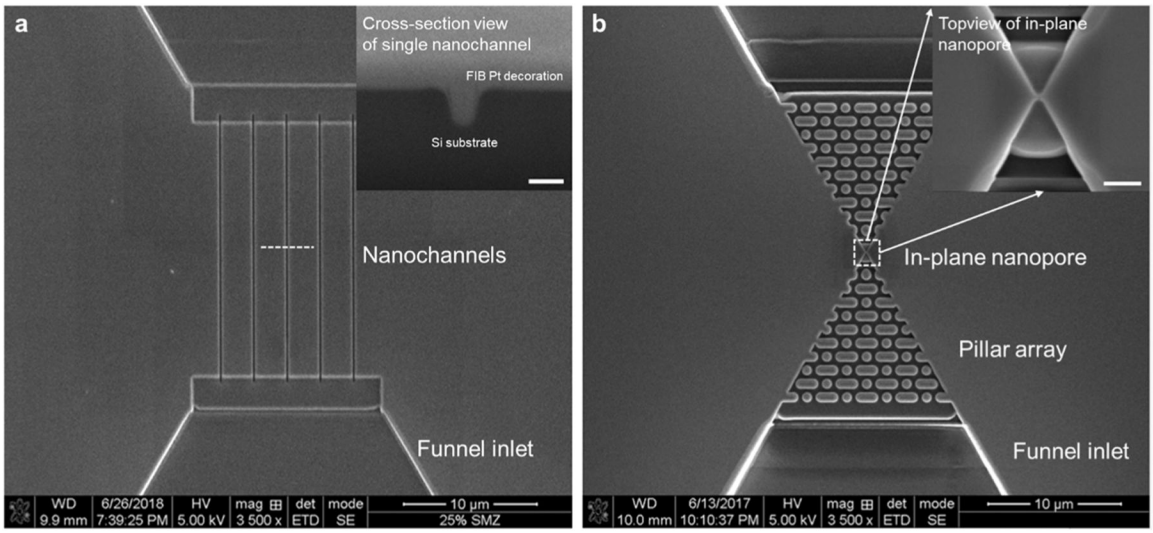

Fig. 2.

(a) Si master mold for thermoplastic nanochannels replication, top-view. It contains five nanochannels with the width, height and length of 154 nm, 203 nm and 20 μm, respectively. Inset, the cross-section SEM image of one of the nanochannels (scale bar 200 nm in white). The structures in the Si master mold were replicated twice to produce final devices in PMMA, COC, and PEGDA. (b) Si master mold containing a single in-plane nanopore for DNA translocation, top-view. Pillar arrays were milled before and after the pore for DNA stretching. Funnel inlet/outlet were built to connect the microchannels. Inset, high magnification SEM image of in-plane nanopore top-view. (scale bar 500 nm in white).

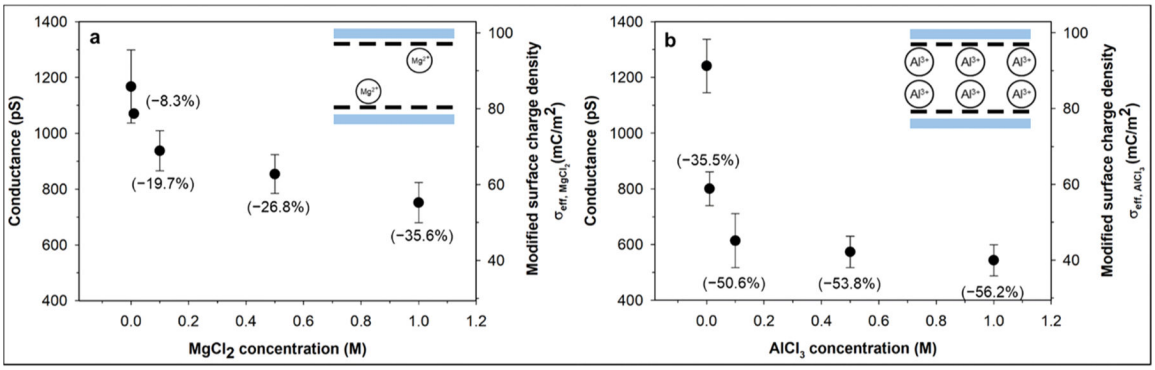

Fig. 3.

Conductance and effective surface charge density of COC nanochannels after modification by $MgCl_2$ (a) and $AlCl_3$ (b), with different ion concentrations of 0 mM, 10 mM, 100 mM, 500 mM and 1 M. The effective surface charge density values were calculated from Eq. (1). Values in brackets indicate the conductance/surface charge density reduction rate in %. The insets illustrate schematics on the electrostatic interaction between the cations and the negatively charged COC surface.

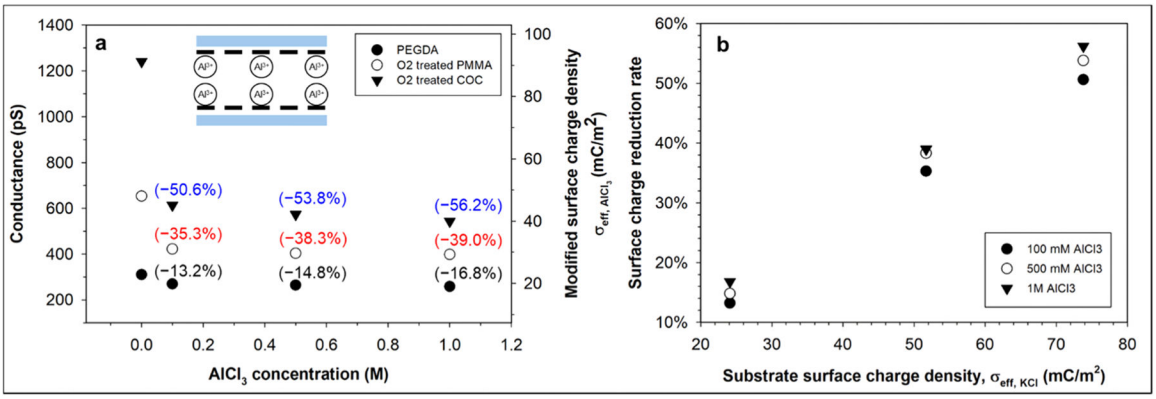

Fig. 4.

(a) Conductance and effective surface charge density of PEGDA-COC, PMMA-COC and COC-COC nanochannels after modification by difference concentration $AlCl_3$ solution. Nanochannel conductance decreases monotonically as $AlCl_3$ concentration increases. Values in brackets indicate conductance/surface charge density reduction rate in %. (b) The surface charge reduction rate upon $AlCl_3$ modification versus the effective surface charge density, $\sigma_{\text{eff, KCl}}$, of different polymers prior to the modification. Nanochannels with more negative surface charge prior to multivalent cation modification resulted in more surface charge reduction due to stronger electrostatic attraction to counterions.

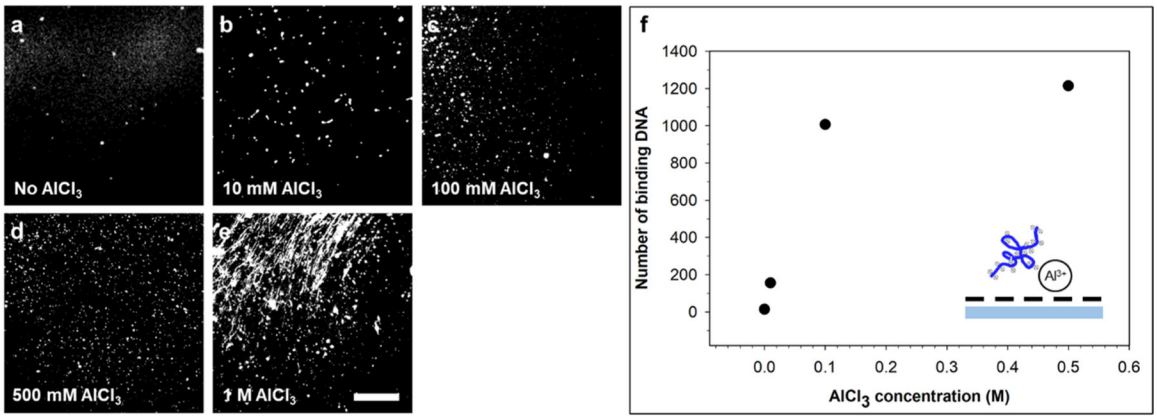

Fig. 5.

λ-DNA binding to Al^{3+} modified COC microchannel wall. (a)-(e) fluorescence image of λ-DNA binding to COC microchannel wall modified by $AlCl_3$ having different concentrations. The scale bar is 15 μm in white. (f) the number of binding DNAs as a function of $AlCl_3$ concentration. Data at 1 M is not available due to a large amount DNA was stuck to COC surface and got stretched during withdraw-and-refill process. Inset illustrates how negatively charged stained DNA binding to Al^{3+} modified COC substrate.

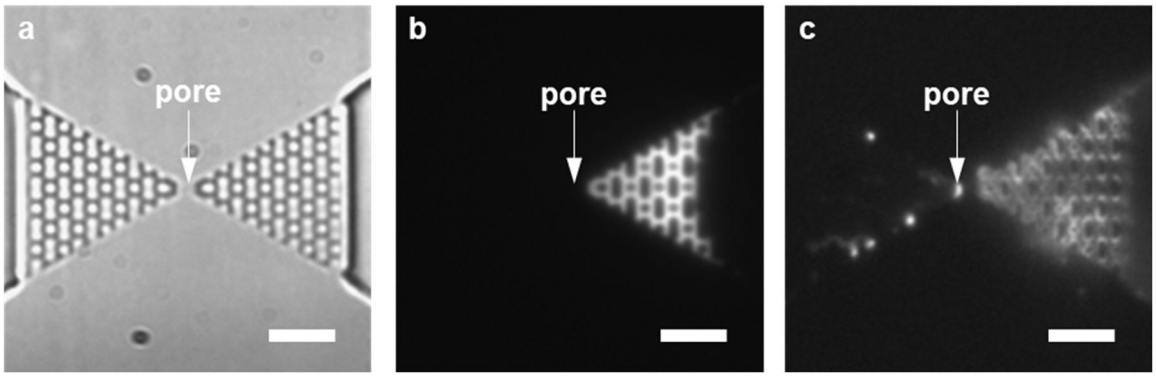

Fig. 6.

DNA translocation through a COC device with an in-plane nanopore. (a) Bright filed top-view image of the COC in-plane nanopore device. (b) Before multivalent ion modification, all the incoming DNA molecules piled up in front of nanopore and no translocation event was observed. (c) After modification by 100 mM $AlCl_3$, DNA translocated through the in-plane nanopore. The results indicated that a surface charge reduction for the COC in-plane nanopore facilitated the translocation of DNA through the nanopore Some DNA molecules were found binding to the pillar structure before and after the nanopore. The image was taken with a 100× oil immersion lens and the scale white scale bar corresponds to 5 μm.